Applied Radiation and Isotopes 177 (2021) 109920

Contents lists available at ScienceDirect

Applied Radiation and Isotopes

journal homepage: www.elsevier.com/locate/apradiso

Photon interaction performance of various contrast agents: Theoretical and simulation results

Mehmet Fatih Turhan

Afyonkarahisar Health Sciences University, Atatürk Vocational School of Health Service, Department of Medical Imaging Techniques, 03200, Afyonkarahisar, Turkey

ARTICLE INFO

Keywords:
Contrast agent
Attenuation coefficient
Effective atomic number
Kerma relative to air
Gamma-ray build-up factor

ABSTRACT

In this study, total mass attenuation coefficient (μ/ρ) values in the energy range from 60 keV to 15 MeV for some contrast agents (Iopamidol, Metrizamide, Iohexol, Ioxaglic acid, Iopromide, Ioversol and Iopentol) were determined with the WinXCOM computer program and GEANT4 computer simulation code. Linear attenuation coefficients (μ), half value layers (*HVL*), tenth value layers (*TVL*), mean free paths (*mfp*), effective atomic numbers (Z_{Eff}) and effective electron densities (N_{Eff}) in the aforementioned energy range were obtained with the help of the calculated total mass attenuation coefficients. Energy absorption build-up factors (*EABF*) and exposure build-up factors (*EBF*) for contrast agents were calculated using the five-parameter geometric progression (G-P) fitting method in the energy region of 0.015 MeV $\leq$ E $\leq$ 15 MeV for different penetration depths up to 40 *mfp* with the help of the equivalent atomic numbers (Z_{eqv}). Kerma relative to air values were investigated in the energy region 0.001 MeV $\leq$ E $\leq$ 20 MeV. It has been observed that Ioxaglic acid is a good radiation absorber according to the other studied contrast agents. The present results may contribute to various application areas of radiation research.

1. Introduction

When monochromatic photons interact with matter, different processes such as photoelectric absorption, Rayleigh scattering, Compton scattering, Delbruck scattering, pair production, etc. Can occur. Photoelectric absorption, Compton scattering and pair production are dominant interactions. By utilizing the interaction cross sections of these processes, the mass attenuation coefficients and related attenuation parameters can be determined both theoretically and experimentally for different materials.

Reliable information about the attenuation parameters is crucial for most application areas such as radiation shields, medical imaging, elemental analysis, etc. Many researchers had been conducted on attenuation properties of different materials. Theoretical and experimental attenuation coefficient, half value layer, tenth value layer, mean free path, effective atomic number, effective electron density, effective removal cross section, radiation protection efficiency, transmission factor, equivalent atomic number, gamma-ray energy absorption and exposure build-up factor values for glass systems (Mahmoud et al., 2019; Kaur et al., 2019; Tekin et al., 2019; Singh et al., 2019), composite materials (Chen et al., 2018; Kökpınar et al., 2020), alloys (Akman et al., 2019a; Sayyed et al., 2019; Manjunatha et al., 2019), ceramics (Akman et al., 2019b; Oto et al., 2019), polymers (Sayyed, 2016; Kaçal et al., 2019) and compounds (Kurudirek et al., 2011; Manjunatha and Rudraswamy, 2012; Ekinci et al., 2014; Kurudirek, 2014; Kavaz et al., 2016; Singh and Badiger, 2016; Issa et al., 2018; Saleh et al., 2019; Yorgun and Kavaz, 2019; Al-Buriahi and Tonguc, 2020; Çakır,2020; Oto et al., 2020) were analyzed. Some of them can be listed as follows. Gamma, neutron shielding and mechanical parameters for some selected alkali lead vanadate glasses were investigated by Mahmoud et al. (2019). Photon attenuation parameters, build-up factors, effective removal cross sections for fast neutrons and proton mass stopping power & proton projected range values for some glasses based on germanium oxide and bismuth oxide were determined by Tekin et al. (2019). Experimental attenuation values were measured at 59.54 keV for ZnO–Al_2O_3–Fe_2O_3–P_2O_5 glasses using the narrow beam transmission geometry by Singh et al. (2019). Chen et al. (2018) calculated the gamma ray shielding parameters for WC_x/Al_{100-x} (x = 10, 20, 50, 80 wt %). Radiation shielding properties were investigated for Poly(hydroxylethyl methacrylate)/Tungsten(VI) oxide composites using the narrow beam transmission geometry by Kökpınar et al. (2020). Radiation shielding and related parameters were experimentally evaluated at different photon energies in the energy region 80.997 keV $\leq$ E $\leq$ 1332.501 keV and theoretical values of the equivalent atomic number and the

E-mail address: m.f.turhan@hotmail.com.

https://doi.org/10.1016/j.apradiso.2021.109920
Received 12 June 2021; Received in revised form 16 August 2021; Accepted 24 August 2021
Available online 28 August 2021

Table 1
Chemical formulas, mass densities and molecular weights of the contrast agents.

Sample Name	Chemical Formula	Density (g/cm^3)	Molecular Weight (g/mol)
Iopamidol	$C_{17}H_{22}I_3N_3O_8$	2.3	777.08
Metrizamide	$C_{18}H_{22}I_3N_3O_8$	2.3	789.09
Iohexol	$C_{19}H_{26}I_3N_3O_9$	2.2	821.14
Ioxaglic acid	$C_{24}H_{21}I_6N_5O_8$	2.5	1268.88
Iopromide	$C_{18}H_{24}I_3N_3O_8$	2.2	791.11
Ioversol	$C_{18}H_{24}I_3N_3O_9$	2.3	807.11
Iopentol	$C_{20}H_{28}I_3N_3O_9$	2.2	835.16

exposure build-up factor were calculated different photon energies ranging from 0.015 MeV to 15 MeV at different penetration depth for binary alloys: Ta95/W5, Ta97.5/W2.5, W72/Cu28, Ta90/W10, In90/Sn10, In95/Sn5, In97/Ag3 and In50/Sn50 by Sayyed et al. (2019). Akman et al. (2019b) and Oto et al. (2019) investigated the different radiation shielding parameters for some selected silicide, boride, oxide types and molybdenum doped ceramics. Kaçal et al. (2019) investigated the radiation attenuation behaviors for Polyamide, Polyacrylonitrile, Polyvinylidenechloride, Polyaniline, Polyethyleneterephthalate, Polyphenylenesulfide, Polypyrrole and Polytetrafluoroethylene. The mass attenuation coefficients, effective atomic numbers, effective electron densities were calculated for some contrast agents by Al-Buriahi and Tonguc (2020) and Çakır (2020). The mass attenuation coefficient, effective atomic number, effective electron density, half value layer (*HVL*) and mean free path values were determined for some selected lanthanide oxides by Issa et al.(2018). Effective atomic numbers, effective electron densities, energy absorption and exposure build-up factor values were calculated using the geometrical progression (G-P) fitting method for hydroxyapatite (HA), cortical bone, some tissue and human organs by Kurudirek et al. (2011), Manjunatha and Rudraswamy (2012) and Saleh et al. (2019). The equivalent atomic numbers, energy absorption build-up factors and exposure build-up factors in the energy range from 0.015 MeV to 15 MeV for penetration depths up to 40 mean free paths were determined for some anti-inflammatory drugs (Ekinci et al., 2014), cancer drugs (Yorgun and Kavaz, 2019), cholinergic drugs (Oto et al., 2020), radio protective agents (Kavaz et al., 2016) and dosimetric materials (Kurudirek, 2014; Singh and Badiger, 2016).

Contrast agent is a material that interacts differently from radiopharmaceuticals with incoming photon; thus, it is used for enhancement of contrast of medical imaging techniques such as magnetic resonance imaging (MRI), mammography, positron emission tomography (PET), computed tomography (CT), etc. Obtaining shielding parameters of these agents may be useful in the above-mentioned practices. In this study, radiation attenuation properties of some selected contrast agents (Iopamidol, Metrizamide, Iohexol, Ioxaglic acid, Iopromide, Ioversol and Iopentol) have been investigated. In order to examine the radiation attenuation parameters; mass attenuation coefficients (μ/ρ), linear attenuation coefficients (μ), half value layers (*HVL*), tenth value layers (*TVL*), mean free paths (*mfp*), effective atomic numbers (Z_{Eff}) and effective electron densities (N_{Eff}) were determined both WinXCOM and GEANT4 in the energy range from 0.06 MeV to 15 MeV for contrast agents. Energy absorption build-up factors (*EABF*) and exposure build-up factors (*EBF*) were calculated using the five-parameter geometric progression (G-P) fitting method in the energy region of 0.015 MeV $\leq$ E $\leq$ 15 MeV for different penetration depths up to 40 *mfp* with the help of the equivalent atomic numbers (Z_{eqv}). Also, kerma relative to air values were investigated in the energy region 0.001 MeV $\leq$ E $\leq$ 20 MeV.

2. Material and methods

2.1. Calculation procedure

The Lambert Beer law describes the attenuation of photon intensity passing through an elemental material and is determined by (Kaçal et al., 2019):

$$I = I_0 e^{-(\mu/\rho)\rho x} \tag{1}$$

where, I and I_0 represent transmitted intensity and the primary intensity, respectively. μ represents the linear attenuation coefficient, ρ represents the density of the absorber and x represents the thickness of the absorber.

Total mass attenuation coefficient (μ/ρ) is derived from eq. (1):

$$\frac{\mu}{\rho} = \frac{1}{\rho x}\ln\left(\frac{I}{I_0}\right) \tag{2}$$

The mass attenuation coefficient for each alloy, mixture or compound is computed using the following equation;

$$\left(\frac{\mu}{\rho}\right)_{Comp} = \sum W_i \left(\frac{\mu}{\rho}\right)_i \tag{3}$$

where, the weight fraction is symbolized with W_i and the mass attenuation coefficient of the ith constituent element is symbolized with $(\mu/\rho)_i$. The weight fraction for an element can be determined as;

$$W_i = \frac{n_i A_i}{\sum_j n_j A_j} \tag{4}$$

A_i is the atomic weight of the ith element and n_i imply the number of atoms of ith constituent element in the compound.

Half Value Layer (*HVL*) and Tenth Value Layer (*TVL*) are the layer thickness required to reduce photon intensity by half and the one tenth as a result of the incoming photon passing through the material, respectively. Mean Free Path (*mfp*) is the average distance between two consecutive collisions. *HVL*, *TVL* and *mfp* are determined using eqs. (5)–(7), respectively (Issa et al., 2018; Kaur et al., 2019). Linear attenuation coefficient (μ) can be determined by the mass attenuation coefficient and physical density of absorber (Table 1).

$$HVL = \frac{\ln 2}{\mu} \tag{5}$$

$$TVL = \frac{\ln 10}{\mu} \tag{6}$$

$$mfp = \frac{1}{\mu} \tag{7}$$

Eqs. (8) and (9) describe the effective atomic number and effective electron density, respectively (Akman et al., 2019a).

$$Z_{Eff} = \frac{\sum_i f_i A_i \left(\mu/\rho\right)_i}{\sum_j f_j \frac{A_j}{Z_j} \left(\mu/\rho\right)_j} \tag{8}$$

$$N_{eff} = \frac{Z_{Eff.}}{A_{tot}} (N n_{tot}) \tag{9}$$

where f_i represents the fractional abundance of the relative element in the material, A_i and Z_i represent the atomic weight and atomic number

Table 2
The comparison of μ/ρ (cm^2/g) results of WinXCOM and GEANT4 for contrast agents.

Energy (MeV)	Iopamidol	Metrizamide	Iohexol	Ioxaglic acid	Iopromide	Ioversol	Iopentol
0.06	3.8087[a]	3.7534[a]	3.6149[a]	4.6213[a]	3.7447[a]	3.6743[a]	3.5575[a]
	3.6476[b]	3.5887[b]	3.4525[b]	4.4360[b]	3.5862[b]	3.5151[b]	3.4034[b]
	4.23[c]	4.39[c]	4.49[c]	4.01[c]	4.23[c]	4.33[c]	4.33[c]
0.08	1.8073[a]	1.7823[a]	1.7199[a]	2.1741[a]	1.7785[a]	1.7466[a]	1.6940[a]
	1.7079[b]	1.6816[b]	1.6195[b]	2.0625[b]	1.6808[b]	1.6474[b]	1.5981[b]
	5.50[c]	5.65[c]	5.84[c]	5.13[c]	5.49[c]	5.68[c]	5.66[c]
0.1	1.0336[a]	1.0201[a]	0.9870[a]	1.2289[a]	1.0183[a]	1.0012[a]	0.9733[a]
	0.9691[b]	0.9551[b]	0.9212[b]	1.1591[b]	0.9548[b]	0.9359[b]	0.9101[b]
	6.24[c]	6.38[c]	6.67[c]	5.68[c]	6.23[c]	6.52[c]	6.49[c]
0.15	0.4145[a]	0.4103[a]	0.4002[a]	0.4749[a]	0.4099[a]	0.4045[a]	0.3960[a]
	0.3850[b]	0.3806[b]	0.3688[b]	0.4467[b]	0.3808[b]	0.3733[b]	0.3658[b]
	7.12[c]	7.23[c]	7.84[c]	5.94[c]	7.09[c]	7.71[c]	7.63[c]
0.2	0.2457[a]	0.2439[a]	0.2397[a]	0.2711[a]	0.2438[a]	0.2415[a]	0.2381[a]
	0.2288[b]	0.2269[b]	0.2208[b]	0.2575[b]	0.2272[b]	0.2227[b]	0.2199[b]
	6.88[c]	6.96[c]	7.89[c]	5.01[c]	6.83[c]	7.78[c]	7.65[c]
0.3	0.1442[a]	0.1437[a]	0.1427[a]	0.1508[a]	0.1438[a]	0.1431[a]	0.1424[a]
	0.1368[b]	0.1361[b]	0.1333[b]	0.1476[b]	0.1365[b]	0.1338[b]	0.1333[b]
	5.19[c]	5.25[c]	6.65[c]	2.10[c]	5.14[c]	6.54[c]	6.37[c]
0.4	0.1110[a]	0.1108[a]	0.1106[a]	0.1128[a]	0.1110[a]	0.1107[a]	0.1106[a]
	0.1071[b]	0.1068[b]	0.1048[b]	0.1132[b]	0.1071[b]	0.1050[b]	0.1051[b]
	3.54[c]	3.61[c]	5.28[c]	−0.40[c]	3.51[c]	5.16[c]	4.99[c]
0.5	0.0945[a]	0.0943[a]	0.0945[a]	0.0945[a]	0.0945[a]	0.0944[a]	0.0946[a]
	0.0922[b]	0.0920[b]	0.0905[b]	0.0965[b]	0.0923[b]	0.0905[b]	0.0908[b]
	2.37[c]	2.43[c]	4.26[c]	−2.13[c]	2.34[c]	4.13[c]	3.98[c]
0.6	0.0841[a]	0.0841[a]	0.0843[a]	0.0835[a]	0.0843[a]	0.0842[a]	0.0844[a]
	0.0828[b]	0.0827[b]	0.0813[b]	0.0862[b]	0.0829[b]	0.0813[b]	0.0817[b]
	1.57[c]	1.64[c]	3.56[c]	−3.28[c]	1.55[c]	3.42[c]	3.28[c]
0.8	0.0711[a]	0.0712[a]	0.0715[a]	0.0700[a]	0.0713[a]	0.0713[a]	0.0716[a]
	0.0707[b]	0.0706[b]	0.0695[b]	0.0732[b]	0.0708[b]	0.0694[b]	0.0698[b]
	0.69[c]	0.77[c]	2.80[c]	−4.58[c]	0.69[c]	2.64[c]	2.52[c]
1	0.0629[a]	0.0629[a]	0.0632[a]	0.0615[a]	0.0630[a]	0.0631[a]	0.0634[a]
	0.0627[b]	0.0626[b]	0.0616[b]	0.0647[b]	0.0628[b]	0.0616[b]	0.0620[b]
	0.33[c]	0.41[c]	2.49[c]	−5.16[c]	0.33[c]	2.33[c]	2.22[c]
1.5	0.0506[a]	0.0507[a]	0.0510[a]	0.0495[a]	0.0508[a]	0.0508[a]	0.0511[a]
	0.0506[b]	0.0506[b]	0.0498[b]	0.0522[b]	0.0507[b]	0.0497[b]	0.0500[b]
	0.12[c]	0.17[c]	2.33[c]	−5.56[c]	0.14[c]	2.16[c]	2.07[c]
2	0.0441[a]	0.0441[a]	0.0444[a]	0.0433[a]	0.0442[a]	0.0443[a]	0.0445[a]
	0.0440[b]	0.0440[b]	0.0433[b]	0.0456[b]	0.0441[b]	0.0433[b]	0.0435[b]
	0.22[c]	0.32[c]	2.41[c]	−5.40[c]	0.25[c]	2.24[c]	2.16[c]
3	0.0374[a]	0.0374[a]	0.0375[a]	0.0372[a]	0.0375[a]	0.0374[a]	0.0375[a]
	0.0372[b]	0.0372[b]	0.0365[b]	0.0389[b]	0.0373[b]	0.0365[b]	0.0367[b]
	0.46[c]	0.56[c]	2.56[c]	−4.84[c]	0.49[c]	2.38[c]	2.32[c]
4	0.0341[a]	0.0340[a]	0.0341[a]	0.0344[a]	0.0341[a]	0.0340[a]	0.0341[a]
	0.0339[b]	0.0338[b]	0.0332[b]	0.0359[b]	0.0339[b]	0.0333[b]	0.0333[b]
	0.50[c]	0.61[c]	2.50[c]	−4.44[c]	0.53[c]	2.33[c]	2.27[c]
5	0.0323[a]	0.0322[a]	0.0321[a]	0.0330[a]	0.0323[a]	0.0322[a]	0.0321[a]
	0.0321[b]	0.0320[b]	0.0314[b]	0.0343[b]	0.0321[b]	0.0315[b]	0.0314[b]
	0.47[c]	0.58[c]	2.37[c]	−4.16[c]	0.49[c]	2.19[c]	2.15[c]
6	0.0312[a]	0.0311[a]	0.0310[a]	0.0323[a]	0.0312[a]	0.0311[a]	0.0309[a]
	0.0311[b]	0.0310[b]	0.0303[b]	0.0335[b]	0.0311[b]	0.0304[b]	0.0303[b]
	0.36[c]	0.48[c]	2.19[c]	−4.00[c]	0.39[c]	2.01[c]	1.98[c]
8	0.0303[a]	0.0302[a]	0.0300[a]	0.0319[a]	0.0302[a]	0.0301[a]	0.0299[a]
	0.0303[b]	0.0301[b]	0.0294[b]	0.0331[b]	0.0301[b]	0.0295[b]	0.0293[b]
	0.30[c]	0.42[c]	1.98[c]	−3.62[c]	0.32[c]	1.81[c]	1.78[c]
10	0.0302[a]	0.0301[a]	0.0297[a]	0.0322[a]	0.0301[a]	0.0299[a]	0.0296[a]
	0.0301[b]	0.0299[b]	0.0292[b]	0.0333[b]	0.0299[b]	0.0294[b]	0.0291[b]
	0.38[c]	0.50[c]	1.95[c]	−3.17[c]	0.40[c]	1.78[c]	1.75[c]
15	0.0310[a]	0.0308[a]	0.0304[a]	0.0339[a]	0.0308[a]	0.0306[a]	0.0302[a]
	0.0308[b]	0.0306[b]	0.0297[b]	0.0346[b]	0.0306[b]	0.0300[b]	0.0296[b]
	0.80[c]	0.92[c]	2.17[c]	−2.15[c]	0.81[c]	2.01[c]	1.98[c]

[a] WinXCOM.
[b] GEANT4.
[c] Relative Deviation (R.D.=$((\mu/\rho_{WinXCOM}- \mu/\rho_{GEANT4})/\mu/\rho_{WinXCOM})$x100).

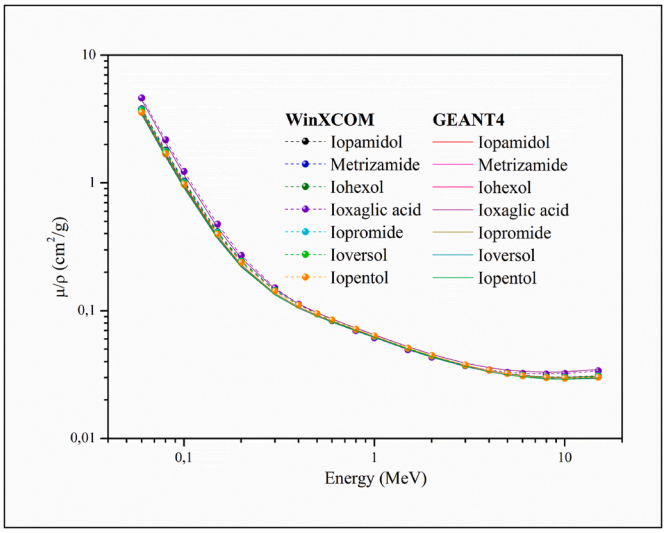

Fig. 1. Total mass attenuation coefficients versus photon energy.

of relative element in the material, respectively. A_{tot}, n_{tot} and N symbolize the total atomic weight of compound, total number of atoms and Avogadro constant, respectively.

2.2. GEANT4 simulation code

The simulations of this study have been carried out by utilizing GEANT4 simulation package (Agostinelli et al., 2003; Aygün et al., 2020). GEANT4, written C++ programming language and based on Monte Carlo method, is a useful toolkit that is applied in various purposes, i.e., high energy physics, nuclear physics, medical and radiation shielding applications. This computer code presents some physical models to handle all electromagnetic and nuclear interactions throughout a wide range of energy. Except for physics model to be used, it is essential to describe the detector geometry and the energy of the primary particle for any calculation. A simple narrow beam geometry consisting of a point gamma source and a slab of the composite is used for the present study. The mono-energetic gamma source has been positioned on one of the edges of the sample such that the momentum directions of the photons are perpendicular to its surface. The calculations have been obtained at photon energy points varying from 0.060 MeV to 15 MeV for ten million photons in each run.

2.3. Calculation of build-up factors

In order to determine the energy absorption build-up factor (*EABF*) and exposure build-up factor (*EBF*) values, the equivalent atomic number (Z_{eqv}) of a given material is firstly calculated with the Geometric Progression (G-P) fitting method. After first step, geometric progression (G-P) fitting coefficients are calculated with the help of the equivalent atomic number (Z_{eqv}). Finally, *EABF* and *EBF* values are determined with the help of the geometric progression (G-P) fitting coefficients for a given material.

In order to determine Z_{eqv}, Compton partial mass attenuation coefficient ($(\mu/\rho)_{Compton}$) and total mass attenuation coefficient ($(\mu/\rho)_{Total}$) were calculated for the elements in the atomic number $18 \leq Z \leq 45$ and contrast agent in the energy range from 0.015 MeV to 15 MeV using the WinXCom program (Gerward et al., 2004). The equivalent atomic number (Z_{eqv}) of the contrast agent was calculated by matching the $(\mu/\rho)_{Compton}/(\mu/\rho)_{Total}$ of the contrast agent at a certain energy with the corresponding ratio of an element at the same energy. When the ratio $(\mu/\rho)_{Compton}/(\mu/\rho)_{Total}$ lies between two successive ratios of elements for a contrast agent, the interpolation of the equivalent atomic number (Z_{eqv}) of a contrast agent is determined with the following equation (Saleh et al., 2019).

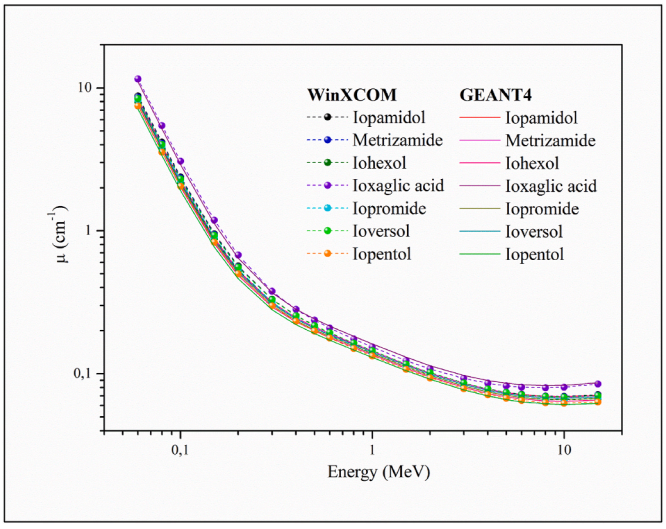

Fig. 2. The linear attenuation coefficients versus photon energy.

Table 3
The comparison of *HVL* (cm) results of WinXCOM and GEANT4 for contrast agents.

Energy (MeV)	Iopamidol	Metrizamide	Iohexol	Ioxaglic acid	Iopromide	Ioversol	Iopentol
0.06	0.079[a]	0.080[a]	0.087[a]	0.060[a]	0.084[a]	0.082[a]	0.093[a]
	0.083[b]	0.084[b]	0.091[b]	0.063[b]	0.088[b]	0.086[b]	0.097[b]
0.08	0.167[a]	0.169[a]	0.183[a]	0.128[a]	0.177[a]	0.173[a]	0.195[a]
	0.176[b]	0.179[b]	0.195[b]	0.134[b]	0.187[b]	0.183[b]	0.207[b]
0.1	0.292[a]	0.295[a]	0.319[a]	0.226[a]	0.309[a]	0.301[a]	0.339[a]
	0.311[b]	0.316[b]	0.342[b]	0.239[b]	0.330[b]	0.322[b]	0.363[b]
0.15	0.727[a]	0.735[a]	0.787[a]	0.584[a]	0.769[a]	0.745[a]	0.833[a]
	0.783[b]	0.792[b]	0.854[b]	0.621[b]	0.827[b]	0.807[b]	0.902[b]
0.2	1.226[a]	1.236[a]	1.314[a]	1.023[a]	1.292[a]	1.248[a]	1.386[a]
	1.317[b]	1.328[b]	1.427[b]	1.077[b]	1.387[b]	1.353[b]	1.501[b]
0.3	2.089[a]	2.098[a]	2.207[a]	1.839[a]	2.190[a]	2.106[a]	2.318[a]
	2.204[b]	2.214[b]	2.364[b]	1.879[b]	2.309[b]	2.253[b]	2.476[b]
0.4	2.715[a]	2.721[a]	2.848[a]	2.459[a]	2.839[a]	2.723[a]	2.984[a]
	2.814[b]	2.822[b]	3.006[b]	2.449[b]	2.942[b]	2.871[b]	3.141[b]
0.5	3.191[a]	3.194[a]	3.335[a]	2.934[a]	3.333[a]	3.193[a]	3.490[a]
	3.268[b]	3.274[b]	3.483[b]	2.872[b]	3.413[b]	3.330[b]	3.635[b]
0.6	3.583[a]	3.585[a]	3.737[a]	3.322[a]	3.739[a]	3.580[a]	3.909[a]
	3.640[b]	3.645[b]	3.875[b]	3.217[b]	3.798[b]	3.707[b]	4.041[b]
0.8	4.235[a]	4.235[a]	4.407[a]	3.962[a]	4.417[a]	4.225[a]	4.607[a]
	4.264[b]	4.268[b]	4.534[b]	3.789[b]	4.447[b]	4.340[b]	4.726[b]
1	4.793[a]	4.792[a]	4.983[a]	4.505[a]	4.997[a]	4.779[a]	5.208[a]
	4.809[b]	4.812[b]	5.111[b]	4.283[b]	5.014[b]	4.340[b]	5.326[b]
1.5	5.950[a]	5.948[a]	6.183[a]	5.606[a]	6.202[a]	5.930[a]	6.460[a]
	5.957[b]	5.958[b]	6.330[b]	5.311[b]	6.211[b]	6.061[b]	6.596[b]
2	6.829[a]	6.828[a]	7.102[a]	6.409[a]	7.120[a]	6.810[a]	7.422[a]
	6.844[b]	6.850[b]	7.277[b]	6.081[b]	7.138[b]	6.966[b]	7.586[b]
3	8.057[a]	8.063[a]	8.407[a]	7.463[a]	8.411[a]	8.052[a]	8.795[a]
	8.095[b]	8.109[b]	8.627[b]	7.119[b]	8.453[b]	8.249[b]	9.004[b]
4	8.837[a]	8.852[a]	9.252[a]	8.070[a]	9.237[a]	8.852[a]	9.691[a]
	8.882[b]	8.906[b]	9.490[b]	7.727[b]	9.287[b]	9.063[b]	9.916[b]
5	9.333[a]	9.356[a]	9.803[a]	8.412[a]	9.767[a]	9.368[a]	10.279[a]
	9.377[b]	9.410[b]	10.041[b]	8.076[b]	9.815[b]	9.578[b]	10.505[b]
6	9.647[a]	9.678[a]	10.162[a]	8.596[a]	10.106[a]	9.702[a]	10.666[a]
	9.682[b]	9.724[b]	10.389[b]	8.266[b]	10.146[b]	9.901[b]	10.880[b]
8	9.932[a]	9.976[a]	10.513[a]	8.688[a]	10.424[a]	10.020[a]	11.052[a]
	9.962[b]	10.018[b]	10.725[b]	8.385[b]	10.457[b]	10.205[b]	11.252[b]
10	9.972[a]	10.026[a]	10.594[a]	8.601[a]	10.480[a]	10.085[a]	11.151[a]
	10.011[b]	10.077[b]	10.805[b]	8.337[b]	10.522[b]	10.268[b]	11.350[b]
15	9.706[a]	9.774[a]	10.375[a]	8.184[a]	10.222[a]	9.855[a]	10.943[a]
	9.785[b]	9.865[b]	10.605[b]	8.012[b]	10.306[b]	10.057[b]	11.163[b]

[a] WinXCOM.
[b] GEANT4.

$$Z_{eqv} = \frac{Z_1(\log R_2 - \log R) + Z_2(\log R - \log R_1)}{\log R_2 - \log R_1} \tag{10}$$

Z_1 and Z_2 are the atomic numbers of the elements corresponding to the ratios R_1 and R_2, respectively. R is the ratio for contrast agent at certain energy.

Geometric progression (G-P) fitting coefficients for a contrast agent were calculated by the interpolation procedure similar to the equivalent atomic number (Z_{eqv}) calculation procedure. G-P fitting coefficients (b, c, a, X_k and d) for the given material are determined as follow.

$$P = \frac{P_1(\log Z_2 - \log Z_{eq}) + P_2(\log Z_{eq} - \log Z_1)}{\log Z_2 - \log Z_1} \tag{11}$$

P_1 and P_2 are the G-P fitting coefficients corresponding to the element atomic numbers Z_1 and Z_2, respectively, at a given energy. The G-P fitting coefficients for elements were taken from the ANSI/-ANS-6.4.3 (1991) standard reference database, which provides the G-P fitting coefficients for elements from beryllium to iron in the energy region 0.015 MeV–15 MeV up to a depth of 40 *mfp*.

To calculate the energy absorption and exposure build-up factors, G-P fitting coefficients were used the following formulas (Singh and Badiger, 2016; Saleh et al., 2019);

$$B(E,x) = 1 + \frac{b-1}{K-1}(K^x - 1) \text{ for } K \neq 1 \tag{12}$$

$$B(E,x) = 1 + (b-1)x \text{ for } K = 1 \tag{13}$$

where,

$$K(E,x) = cx^a + d\frac{\tanh(x/X_k - 2) - \tanh(-2)}{1 - \tanh(-2)} \text{ for } x \leq 40\ mfp \tag{14}$$

the incident photon energy is symbolized with E; the penetration depth in *mfp* is symbolized with x; the G-P fitting coefficients are symbolized with b, c, a, X_k and d, the value of build-up factor at 1*mfp* is symbolized with b.

Table 4
The comparison of *mfp* (cm) results of WinXCOM and GEANT4 for contrast agents.

Energy (MeV)	Iopamidol	Metrizamide	Iohexol	Ioxaglic acid	Iopromide	Ioversol	Iopentol
0.06	0.114[a]	0.116[a]	0.126	0.087[a]	0.121[a]	0.118[a]	0.134[a]
	0.119[b]	0.121[b]	0.132[b]	0.090[b]	0.127[b]	0.124[b]	0.140[b]
0.08	0.241[a]	0.244[a]	0.264[a]	0.184[a]	0.256[a]	0.249[a]	0.281[a]
	0.255[b]	0.259[b]	0.281[b]	0.194[b]	0.270[b]	0.264[b]	0.298[b]
0.1	0.421[a]	0.426[a]	0.461[a]	0.325[a]	0.446[a]	0.434[a]	0.489[a]
	0.449[b]	0.455[b]	0.493[b]	0.345[b]	0.476[b]	0.465[b]	0.523[b]
0.15	1.049[a]	1.060[a]	1.136[a]	0.842[a]	1.109[a]	1.075[a]	1.202[a]
	1.129[b]	1.142[b]	1.232[b]	0.895[b]	1.194[b]	1.165[b]	1.302[b]
0.2	1.769[a]	1.783[a]	1.896[a]	1.476[a]	1.864[a]	1.801[a]	2.000[a]
	1.900[b]	1.916[b]	2.059[b]	1.554[b]	2.001[b]	1.952[b]	2.166[b]
0.3	3.014[a]	3.026[a]	3.184[a]	2.653[a]	3.160[a]	3.038[a]	3.344[a]
	3.179[b]	3.194[b]	3.411[b]	2.710[b]	3.331[b]	3.251[b]	3.572[b]
0.4	3.917[a]	3.925[a]	4.108[a]	3.547[a]	4.096[a]	3.929[a]	4.305[a]
	4.060[b]	4.072[b]	4.337[b]	3.533[b]	4.245[b]	4.142[b]	4.531[b]
0.5	4.603[a]	4.609[a]	4.811[a]	4.232[a]	4.808[a]	4.606[a]	5.035[a]
	4.715[b]	4.724[b]	5.025[b]	4.144[b]	4.923[b]	4.804[b]	5.244[b]
0.6	5.169[a]	5.172[a]	5.391[a]	4.793[a]	5.395[a]	5.165[a]	5.639[a]
	5.251[b]	5.258[b]	5.590[b]	4.641[b]	5.480[b]	5.348[b]	5.830[b]
0.8	6.109[a]	6.110[a]	6.358[a]	5.717[a]	6.372[a]	6.096[a]	6.647[a]
	6.152[b]	6.157[b]	6.541[b]	5.466[b]	6.416[b]	6.261[b]	6.819[b]
1	6.915[a]	6.914[a]	7.190[a]	6.499[a]	7.210[a]	6.895[a]	7.513[a]
	6.938[b]	6.943[b]	7.373[b]	6.180[b]	7.234[b]	7.059[b]	7.684[b]
1.5	8.584[a]	8.581[a]	8.920[a]	8.088[a]	8.948[a]	8.555[a]	9.319[a]
	8.595[b]	8.596[b]	9.132[b]	7.662[b]	8.961[b]	8.744[b]	9.516[b]
2	9.852[a]	9.851[a]	10.246[a]	9.247[a]	10.272[a]	9.824[a]	10.708[a]
	9.874[b]	9.882[b]	10.499[b]	8.773[b]	10.298[b]	10.050[b]	10.945[b]
3	11.624[a]	11.633[a]	12.128[a]	10.766[a]	12.135[a]	11.617[a]	12.689[a]
	11.678[b]	11.699[b]	12.446[b]	10.270[b]	12.195[b]	11.900[b]	12.990[b]
4	12.749[a]	12.770[a]	13.348[a]	11.642[a]	13.327[a]	12.770[a]	13.981[a]
	12.814[b]	12.849[b]	13.691[b]	11.147[b]	13.398[b]	13.075[b]	14.306[b]
5	13.465[a]	13.498[a]	14.143[a]	12.136[a]	14.091[a]	13.516[a]	14.829[a]
	13.528[b]	13.576[b]	14.486[b]	11.651[b]	14.161[b]	13.819[b]	15.155[b]
6	13.918[a]	13.962[a]	14.661[a]	12.402[a]	14.580[a]	13.997[a]	15.387[a]
	13.968[b]	14.029[b]	14.989[b]	11.925[b]	14.637[b]	14.284[b]	15.697[b]
8	14.329[a]	14.393[a]	15.167[a]	12.534[a]	15.038[a]	14.456[a]	15.944[a]
	14.373[b]	14.453[b]	15.473[b]	12.096[b]	15.087[b]	14.722[b]	16.233[b]
10	14.387[a]	14.465[a]	15.285[a]	12.409[a]	15.119[a]	14.550[a]	16.088[a]
	14.442[b]	14.538[b]	15.589[b]	12.027[b]	15.180[b]	14.813[b]	16.375[b]
15	14.003[a]	14.100[a]	14.968[a]	11.806[a]	14.748[a]	14.218[a]	15.787[a]
	14.116[b]	14.232[b]	15.299[b]	11.558[b]	14.869[b]	14.510[b]	16.105[b]

[a] WinXCOM.
[b] GEANT4.

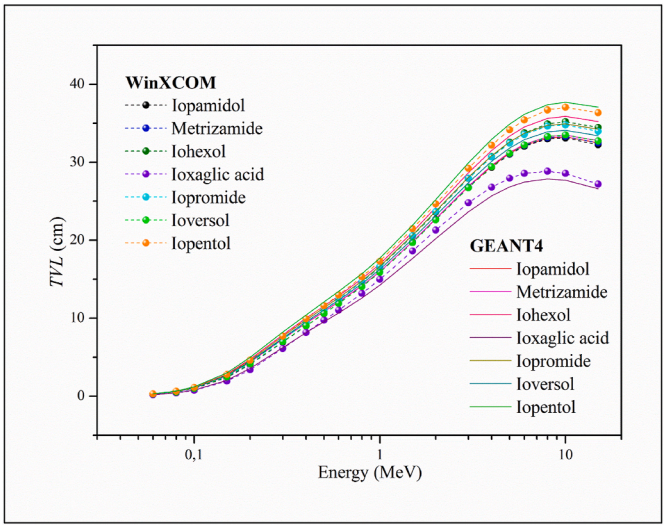

Fig. 3. *TVL* values versus photon energy.

Table 5
The comparison of Z_{Eff} results of WinXCOM and GEANT4 for contrast agents.

Energy (MeV)	Iopamidol	Metrizamide	Iohexol	Ioxaglic acid	Iopromide	Ioversol	Iopentol
0.06	41.24[a]	41.07[a]	40.02[a]	45.44[a]	40.71[a]	40.54[a]	39.52[a]
	39.50[b]	39.27[b]	38.23[b]	43.62[b]	38.99[b]	38.78[b]	37.81[b]
0.08	34.08[a]	33.86[a]	32.51[a]	39.96[a]	33.37[a]	33.17[a]	31.87[a]
	32.20[b]	31.95[b]	30.61[b]	37.91[b]	31.54[b]	31.29[b]	30.07[b]
0.1	27.67[a]	27.44[a]	26.03[a]	34.33[a]	26.92[a]	26.72[a]	25.38[a]
	25.94[b]	25.69[b]	24.30[b]	32.38[b]	25.24[b]	24.98[b]	23.73[b]
0.15	17.45[a]	17.28[a]	16.15[a]	23.51[a]	16.83[a]	16.71[a]	15.64[a]
	16.21[b]	16.03[b]	14.89[b]	22.11[b]	15.64[b]	15.42[b]	14.45[b]
0.2	12.80[a]	12.69[a]	11.83[a]	17.62[a]	12.32[a]	12.26[a]	11.44[a]
	11.92[b]	11.81[b]	10.90[b]	16.74[b]	11.48[b]	11.30[b]	10.57[b]
0.3	9.39[a]	9.33[a]	8.73[a]	12.82[a]	9.05[a]	9.03[a]	8.45[a]
	8.90[b]	8.84[b]	8.15[b]	12.55[b]	8.58[b]	8.44[b]	7.91[b]
0.4	8.28[a]	8.23[a]	7.73[a]	11.16[a]	7.98[a]	7.98[a]	7.49[a]
	7.98[b]	7.94[b]	7.32[b]	11.20[b]	7.70[b]	7.57[b]	7.12[b]
0.5	7.80[a]	7.76[a]	7.29[a]	10.42[a]	7.53[a]	7.53[a]	7.08[a]
	7.61[b]	7.57b	6.98[b]	10.64[b]	7.35[b]	7.22[b]	6.80[b]
0.6	7.55[a]	7.52[a]	7.07[a]	10.04[a]	7.29[a]	7.30[a]	6.87[a]
	7.43[b]	7.40[b]	6.82[b]	10.37[b]	7.18[b]	7.05[b]	6.64[b]
0.8	7.31[a]	7.29[a]	6.86[a]	9.67[a]	7.06[a]	7.08[a]	6.66[a]
	7.26[b]	7.23[b]	6.67[b]	10.11[b]	7.01[b]	6.89[b]	6.49[b]
1	7.20[a]	7.18[a]	6.76[a]	9.50[a]	6.96[a]	6.98[a]	6.57[a]
	7.18[b]	7.15[b]	6.59[b]	9.99[b]	6.93[b]	6.81[b]	6.42[b]
1.5	7.14[a]	7.12[a]	6.71[a]	9.40[a]	6.90[a]	6.92[a]	6.52[a]
	7.13[b]	7.11[b]	6.55[b]	9.92[b]	6.89[b]	6.77[b]	6.38[b]
2	7.25[a]	7.22[a]	6.80[a]	9.56[a]	7.00[a]	7.02[a]	6.61[a]
	7.23[b]	7.20[b]	6.64[b]	10.08[b]	6.99[b]	6.86[b]	6.47[b]
3	7.64[a]	7.61[a]	7.16[a]	10.15[a]	7.38[a]	7.39[a]	6.95[a]
	7.60[b]	7.57[b]	6.98[b]	10.64[b]	7.34[b]	7.22[b]	6.79[b]
4	8.12[a]	8.08[a]	7.59[a]	10.86[a]	7.84[a]	7.84[a]	7.37[a]
	8.08[b]	8.03[b]	7.40[b]	11.34[b]	7.80[b]	7.66[b]	7.20[b]
5	8.62[a]	8.58[a]	8.05[a]	11.60[a]	8.33[a]	8.32[a]	7.81[a]
	8.58[b]	8.53[b]	7.86[b]	12.08[b]	8.28[b]	8.14[b]	7.64[b]
6	9.13[a]	9.07[a]	8.51[a]	12.32[a]	8.81[a]	8.80[a]	8.26[a]
	9.10[b]	9.03[b]	8.33[b]	12.81[b]	8.78[b]	8.62[b]	8.09[b]
8	10.11[a]	10.03[a]	9.41[a]	13.68[a]	9.76[a]	9.72[a]	9.12[a]
	10.08[b]	9.99[b]	9.22[b]	14.18[b]	9.72[b]	9.55[b]	8.96[b]
10	11.02[a]	10.93[a]	10.25[a]	14.92[a]	10.64[a]	10.59[a]	9.94[a]
	10.98[b]	10.87[b]	10.05[b]	15.39[b]	10.59[b]	10.40[b]	9.76[b]
15	12.93[a]	12.80[a]	12.02[a]	17.40[a]	12.49[a]	12.41[a]	11.67[a]
	12.82[b]	12.68[b]	11.76[b]	17.78[b]	12.39[b]	12.16[b]	11.44[b]

[a] WinXCOM.
[b] GEANT4.

2.4. Calculation of kerma relative to air

Kerma is the expectation value of the energy transferred to charged particles per unit mass at a point of interest, including radiative-loss energy but excluding energy passed from one charged particle to another (Attix, 1986). Kerma at an interested point is associated to energy fluence and mass energy absorption coefficient and determined the following equation.

$$K = \Psi\left(\frac{\mu_{en}}{\rho}\right) \tag{15}$$

Here Ψ is the energy fluence, μ_{en} is the linear energy transfer coefficient and ρ is the density of the absorber. Kerma relative to air values of a contrast agent can be computed using the following equation.

$$\frac{(\mu_{en}/\rho)_{CA}}{(\mu_{en}/\rho)_{Air}} \tag{16}$$

The mass energy absorption coefficient for a contrast agent is determined with the help of equation (17).

$$\left(\frac{\mu_{en}}{\rho}\right)_{CA} = \sum W_i \left(\frac{\mu_{en}}{\rho}\right)_i \tag{17}$$

Where, the weight fraction is symbolized with W_i and the mass energy absorption coefficient of the *ith* constituent element is symbolized with $(\mu_{en}/\rho)_i$.

3. Results and discussion

3.1. Results of photon attenuation parameters

Chemical formulas, mass densities and molecular weights for contrast agents (Eng et al., 2015) are given in Table 1. Total mass attenuation coefficients and linear attenuation coefficients for contrast agents in the energy region 60 keV ≤ E ≤ 15 MeV are listed Table 2 and plotted as a function of energy in Fig. 1 and Fig. 2, respectively. As seen from Table 2, Figs. 1 and 2, total mass attenuation coefficient and linear attenuation coefficient values are very close each other for contrast agents. The differences between WinXCOM and GEANT4 simulation codes of μ/ρ values for Iopamidol, Metrizamide, Iohexol, Ioxaglic acid, Iopromide, Ioversol and Iopentol are <7.2%, <7.3%, <7.9%, <6%, <7.1%, <7.8% and <7.7%, respectively. This consistency is a powerful sign in terms of the accuracy of μ/ρ values reported in this study. Ioxaglic acid is the contrast agent that takes the maximum total mass and

Table 6
The comparison of N_{Eff} (x10^{23}) results of WinXCOM and GEANT4 for contrast agents.

Energy (MeV)	Iopamidol	Metrizamide	Iohexol	Ioxaglic acid	Iopromide	Ioversol	Iopentol
0.06	77.46[a]	78.60[a]	85.10[a]	103.06[a]	80.79[a]	81.89[a]	88.24[a]
	74.19[b]	75.15[b]	81.28[b]	98.93[b]	77.37[b]	78.34[b]	84.42[b]
0.08	64.00[a]	64.79[a]	69.12[a]	90.64[a]	66.23[a]	67.01[a]	71.16[a]
	60.48[b]	61.13[b]	65.09[b]	85.99[b]	62.59[b]	63.20[b]	67.13[b]
0.1	51.96[a]	52.52[a]	55.35[a]	77.87[a]	53.42[a]	53.98[a]	56.66[a]
	48.72[b]	49.17[b]	51.66[b]	73.45[b]	50.09[b]	50.46[b]	52.98[b]
0.15	32.77[a]	33.07[a]	34.35[a]	53.32[a]	33.40[a]	33.75[a]	34.92[a]
	30.44[b]	30.68[b]	31.66[b]	50.15[b]	31.03[b]	31.15[b]	32.26[b]
0.2	24.04[a]	24.28[a]	25.16[a]	39.96[a]	24.46[a]	24.76[a]	25.55[a]
	22.39[b]	22.59[b]	23.17[b]	37.96[b]	22.79[b]	22.83[b]	23.60[b]
0.3	17.64[a]	17.85[a]	18.56[a]	29.08[a]	17.96[a]	18.24[a]	18.87[a]
	16.72[b]	16.92[b]	17.32[b]	28.47[b]	17.03[b]	17.05[b]	17.67[b]
0.4	15.54[a]	15.76[a]	16.43[a]	25.30[a]	15.84[a]	16.13[a]	16.72[a]
	14.99[b]	15.19[b]	15.56[b]	25.40[b]	15.29[b]	15.30[b]	15.89[b]
0.5	14.64[a]	14.86[a]	15.51[a]	23.64[a]	14.94[a]	15.22[a]	15.80[a]
	14.30[b]	14.49[b]	14.85[b]	24.14[b]	14.59[b]	14.59[b]	15.17[b]
0.6	14.18[a]	14.39[a]	15.04[a]	22.77[a]	14.47[a]	14.75[a]	15.33[a]
	13.96[b]	14.16[b]	14.50[b]	23.52[b]	14.24[b]	14.25[b]	14.83[b]
0.8	13.73[a]	13.94[a]	14.59[a]	21.93[a]	14.02[a]	14.30[a]	14.87[a]
	13.63[b]	13.83[b]	14.18[b]	22.93[b]	13.92[b]	13.92[b]	14.50[b]
1	13.52[a]	13.73[a]	14.38[a]	21.54[a]	13.81[a]	14.09[a]	14.66[a]
	13.48[b]	13.68[b]	14.02[b]	22.65[b]	13.76[b]	13.76[b]	14.34[b]
1.5	13.41[a]	13.62[a]	14.26[a]	21.32[a]	13.69[a]	13.98[a]	14.55[a]
	13.39[b]	13.60[b]	13.93[b]	22.50[b]	13.67[b]	13.68[b]	14.25[b]
2	13.61[a]	13.82[a]	14.47[a]	21.68[a]	13.90[a]	14.18[a]	14.76[a]
	13.58[b]	13.78[b]	14.12[b]	22.86[b]	13.86[b]	13.86[b]	14.44[b]
3	14.35[a]	14.56[a]	15.23[a]	23.02[a]	14.65[a]	14.93[a]	15.52[a]
	14.28[b]	14.48[b]	14.84[b]	24.14[b]	14.58[b]	14.57[b]	15.16[b]
4	15.25[a]	15.46[a]	16.15[a]	24.63[a]	15.56[a]	15.84[a]	16.45[a]
	15.17[b]	15.37[b]	15.74[b]	25.72[b]	15.48[b]	15.47[b]	16.08[b]
5	16.20[a]	16.41[a]	17.13[a]	26.30[a]	16.52[a]	16.81[a]	17.44[a]
	16.12[b]	16.32[b]	16.72[b]	27.39[b]	16.44[b]	16.44[b]	17.07[b]
6	17.15[a]	17.36[a]	18.10[a]	27.93[a]	17.49[a]	17.77[a]	18.43[a]
	17.08[b]	17.28[b]	17.71[b]	29.05[b]	17.42[b]	17.41[b]	18.07[b]
8	18.99[a]	19.20[a]	20.01[a]	31.04[a]	19.36[a]	19.64[a]	20.37[a]
	18.93[b]	19.12[b]	19.61[b]	32.16[b]	19.30[b]	19.29[b]	20.01[b]
10	20.69[a]	20.91[a]	21.79[a]	33.84[a]	21.11[a]	21.39[a]	22.19[a]
	20.61[b]	20.80[b]	21.37[b]	34.91[b]	21.02[b]	21.01[b]	21.80[b]
15	24.28[a]	24.50[a]	25.56[a]	39.47[a]	24.79[a]	25.07[a]	26.05[a]
	24.09[b]	24.28[b]	25.01[b]	40.32[b]	24.59[b]	24.56[b]	25.53[b]

[a] WinXCOM.
[b] GEANT4.

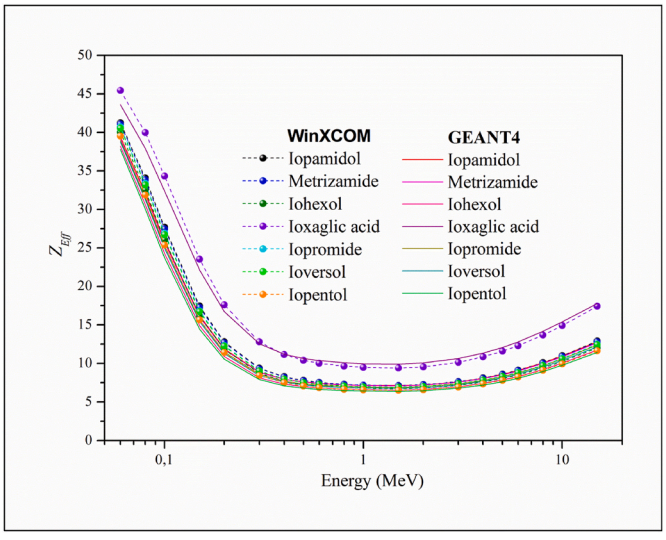

Fig. 4. Z_{Eff} values versus photon energy.

Table 7
Equivalent atomic numbers of the contrast agents for the energy range from 0.015 MeV to 15 MeV.

Energy (MeV)	Iopamidol	Metrizamide	Iohexol	Ioxaglic acid	Iopromide	Ioversol	Iopentol
0.015	19.483	19.361	19.002	21.406	19.311	19.165	18.855
0.02	19.882	19.767	19.433	21.718	19.723	19.584	19.286
0.03	20.447	20.332	20.003	22.201	20.291	20.151	19.867
0.04	37.118	36.895	36.256	40.613	36.819	36.539	35.981
0.05	37.922	37.704	37.075	41.350	37.630	37.353	36.810
0.06	38.461	38.241	37.622	41.822	38.167	37.890	37.360
0.08	39.183	38.969	38.359	42.458	38.899	38.628	38.097
0.1	39.651	39.442	38.840	42.863	39.372	39.103	38.586
0.15	40.349	40.145	39.563	43.453	40.077	39.817	39.316
0.2	40.758	40.557	39.985	43.793	40.491	40.235	39.740
0.3	41.220	41.028	40.460	44.171	40.964	40.708	40.221
0.4	41.463	41.271	40.715	44.375	41.208	40.962	40.477
0.5	41.609	41.418	40.872	44.497	41.355	41.112	40.635
0.6	41.715	41.524	40.987	44.579	41.462	41.220	40.750
0.8	41.814	41.623	41.084	44.659	41.560	41.318	40.851
1	41.849	41.657	41.117	44.688	41.595	41.351	40.886
1.5	39.612	39.378	38.706	43.090	39.298	39.008	38.415
2	34.246	33.930	33.014	39.046	33.810	33.423	32.613
3	29.225	28.885	27.913	34.632	28.751	28.354	27.488
4	27.643	27.309	26.352	33.062	27.174	26.788	25.933
5	26.889	26.559	25.614	32.269	26.424	26.044	25.200
6	26.365	26.038	25.111	31.751	25.905	25.535	24.702
8	25.830	25.506	24.579	31.170	25.372	24.999	24.173
10	25.588	25.266	24.362	30.901	25.132	24.772	23.966
15	25.453	25.130	24.220	30.776	24.996	24.637	23.817

linear attenuation coefficients in the energy range from 60 keV to 15 MeV. As seen from Table 2, Figs. 1 and 2, the values of the total mass and linear attenuation coefficient decreased with increasing photon energy. Reduction of the total mass and linear attenuation coefficients continuous at a slower rate in the low and intermediate energy region, although the values are almost stable in the high energy region. The present results are generally in the good agreement each other. Also, total mass and linear attenuation coefficient values showed similar behaviors with other studies for different materials (Sayyed, 2016; Manjunatha et al., 2019).

Half Value Layer (*HVL*), Tenth Value Layer (*TVL*) and Mean Free Path (*mfp*) provide important information about the radiation attenuation behaviors of the material. In order to determine the *HVL*, *TVL*, *mfp*, linear attenuation coefficient values the energy region 60 keV $\leq$ E $\leq$ 15 MeV were used in eqs. (5)–(7) for contrast agents, respectively. *HVL*, *mfp* values for contrast agents are listed in Table 3 and Table 4, respectively. *TVL* values are plotted against photon energy in Fig. 3. The differences between WinXCOM and GEANT4 simulation codes of *HVL*, *TVL* and *mfp* values for contrast agents are found to be <8.6%. As seen from Tables 3 and 4 and Fig. 3, *HVL*, *TVL* and *mfp* values are increase with increasing photon energy and take the maximum values around the 8–10 MeV energy. After 10 MeV energy, the *HVL*, *TVL* and *mfp* values are entered a decreasing trend. The values of *HVL*, *TVL* and *mfp* could be listed as: Ioxaglic acid < Iopamidol < Metrizamide < Ioversol < Iopromide < Iohexol < Iopentol. As shown Table 3, Table 4 and Fig. 3, half value layer (*HVL*), tenth value layer (*TVL*) and mean free path (*mfp*) values in the energy region 60 keV $\leq$ E $\leq$ 15 MeV found to be 0.093–11.35 cm, 0.308–37.084 cm and 0.134–16.375 cm for Iopentol, respectively. Also, *HVL*, *TVL* and *mfp* values in the energy region 60 keV $\leq$ E $\leq$ 15 MeV found to be 0.060 cm–8.688 cm, 0.199 cm–28.860 cm and 0.087 cm–12.534 cm for Ioxaglic acid, respectively.

Atomic number is not defined as a single number for a material containing more than one element. The atomic number value can be defined as effective atomic number (Z_{Eff}) and it can take different values at different energies for a material. The number of electrons per unit mass is expressed with the effective electron density (N_{Eff}). Effective

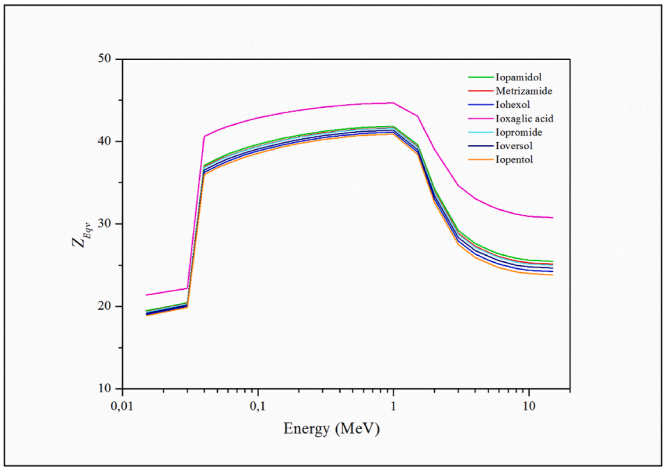

Fig. 5. Z_{eqv} values versus photon energy.

Table 8
G-P energy absorption and exposure build-up factor coefficients of the Iopamidol in the energy range from 0.015 MeV to 15 MeV.

	EABF					EBF				
Energy (MeV)	a	b	c	d	Xk	a	b	c	d	Xk
0.015	0.232	1.008	0.400	−0.168	11.391	0.327	1.010	0.358	−0.252	9.258
0.02	0.261	1.018	0.356	−0.186	11.390	0.193	1.017	0.423	−0.092	11.062
0.03	0.238	1.054	0.359	−0.150	13.312	0.223	1.055	0.372	−0.135	13.020
0.04	0.137	1.339	0.344	−0.126	23.964	0.138	2.974	0.325	−0.053	20.394
0.05	−0.044	1.297	0.135	0.049	9.566	−0.163	2.547	0.125	0.002	12.216
0.06	0.668	1.278	0.098	−0.181	14.820	0.897	2.099	0.090	−0.145	16.574
0.08	0.506	1.290	0.140	−0.208	14.106	0.659	1.573	0.110	−0.229	14.319
0.1	0.298	1.223	0.297	−0.156	14.665	0.271	1.178	0.332	−0.146	13.772
0.15	0.278	1.520	0.337	−0.157	14.036	0.166	1.271	0.510	−0.086	14.373
0.2	0.302	2.306	0.336	−0.190	13.983	0.163	1.492	0.540	−0.094	14.236
0.3	0.153	2.413	0.577	−0.095	13.996	0.076	1.603	0.748	−0.042	14.390
0.4	0.102	2.682	0.726	−0.085	13.850	0.036	1.718	0.899	−0.033	14.085
0.5	0.065	2.694	0.838	−0.063	13.841	0.015	1.776	0.983	−0.023	14.219
0.6	0.046	2.649	0.897	−0.053	13.704	0.003	1.798	1.028	−0.018	13.840
0.8	0.024	2.501	0.969	−0.039	13.602	−0.008	1.805	1.075	−0.013	13.936
1	0.014	2.367	1.003	−0.031	13.487	−0.013	1.784	1.093	−0.010	13.372
1.5	−0.013	1.943	1.102	−0.014	12.634	−0.031	1.641	1.165	0.002	8.905
2	−0.009	1.842	1.084	−0.014	11.097	−0.021	1.653	1.124	−0.005	10.570
3	0.002	1.674	1.039	−0.018	12.290	−0.004	1.616	1.059	−0.015	12.223
4	0.012	1.552	1.007	−0.029	14.023	0.007	1.549	1.059	−0.023	12.924
5	0.022	1.468	0.976	−0.038	14.143	0.013	1.482	1.025	−0.027	13.163
6	0.023	1.392	0.978	−0.038	14.326	0.023	1.440	1.009	−0.036	13.352
8	0.033	1.300	0.957	−0.044	13.960	0.029	1.355	0.973	−0.042	13.647
10	0.038	1.237	0.955	−0.048	14.248	0.042	1.298	0.948	−0.055	13.947
15	0.046	1.150	0.955	−0.052	14.617	0.049	1.200	0.954	−0.059	14.333

atomic number (Z_{Eff}) and effective electron density (N_{Eff}) were calculated using eqs. (8) and (9) in the energy region 60 keV ≤ E ≤ 15 MeV for Iopamidol, Metrizamide, Iohexol, Ioxaglic acid, Iopromide, Ioversol and Iopentol. The change of effective atomic number and effective electron density values both WinXCOM and GEANT4 simulation codes versus photon energy for contrast agents are listed in Table 5 and Table 6, respectively. Besides, Fig. 4 shows the results for Z_{Eff} as a function of energy up to 15 MeV. The highest Z_{Eff} and N_{Eff} values were found for Ioxaglic acid among the selected contrast agents. Z_{Eff} and N_{Eff} values in the energy region 60 keV ≤ E ≤ 15 MeV are found to be between 45.44 and 9.40 and 103.06×10^{23} - 21.32×10^{23} for Ioxaglic acid, respectively. As seen from Table 5, Table 6 and Fig. 4, the agreement WinXCOM and GEANT4 looked pretty good for both Z_{Eff} and N_{Eff} values. The differences between WinXCOM and GEANT4 simulation codes of Z_{Eff} and N_{Eff} values for contrast agents are <7.9%. Besides, Z_{Eff} and N_{Eff} values of the contrast agents showed different behaviors at different energy region just like Figs. 1–3. Z_{Eff} and N_{Eff} values were abruptly decreased with increasing photon energy up to ~400 keV. The contribution of photoelectric effect is clearly seen for contrast agents. Also, Compton scattering effect is dominant with respect to photoelectric effect in the intermediate energy region. The differences between the values of the contrast agents increase with increasing energy at each energy point in the high energy region. Increasing these differences are evidence that pair production effect is more dominant at higher energies. The values of *HVL*, *TVL*, *mfp*, Z_{Eff} and N_{Eff} showed same behavior for different materials such as glass (Kaur et al., 2019; Tekin et al., 2019), alloys (Manjunatha et al., 2019) and compounds (Singh and Badiger, 2016; Issa et al., 2018; Oto et al., 2020).

3.2. Results of build-up factors

Equivalent atomic numbers (Z_{eqv}) calculated from eq. (10) in the energy region 0.015 MeV ≤ E ≤ 15 MeV for selected contrast agents were tabulated in Table 7 and plotted in Fig. 5. Geometric progressing (G-P) energy absorption build-up factor coefficients and exposure build-up factor coefficients were calculated from eq. (11). Also, G-P energy absorption and exposure build-up coefficients in the energy range from 0.015 MeV to 15 MeV for Iopamidol were listed in Table 8. In order to determine the energy absorption build-up factors (*EABF*) and exposure build-up factors (*EBF*), G-P fitting coefficients and penetration depths were used in eqs. (12)–(14). Energy absorption build-up factor values of some selected contrast agents are plotted in Fig. 6(a–h) against the incident photon energy in the energy region 0.015 MeV ≤ E ≤ 15 MeV at 0.5, 1, 2, 5, 10, 20, 30 and 40 *mfp*. Fig. 7(a–h) shows the exposure build-up factor (*EBF*) values of the contrast agents according to the incident photon energy in the energy range from 0.015 MeV to 15 MeV for penetration depths 0.5, 1, 2, 5, 10, 20, 30 and 40 *mfp*.

As seen from Fig. 6(a–h) and 7 (a-h), Ioxaglic acid generally received the lowest *EABF* and *EBF* values at the low energy region and intermediate energy region except for around the Iodine K shell absorption edge energy at low penetration depths. It is obviously seen chemical formulas from Table 1, the contribution of iodine is higher in Ioxaglic acid ($C_{24}H_{21}I_6N_5O_8$) than other compounds. A very sharp peak can be seen from Fig. 6(a–h) and 7 (a-h), at 0.06 MeV for *EABF* and *EBF* values for the contrast agents due to penetration depths and Z_{eqv}. The *EABF* and *EBF* values for Iopentol are generally found largest (Figs. 6 and 7) at especially high penetration depths at 0.06 MeV because of high Z_{eqv} value among the contrast agents.

As seen from Figs. 6 and 7 just like Figs. 1–5, photoelectric absorption dominates in the region of low energy. It is clearly seen from Figs. 6 and 7, this effect is generally more dominant for Ioxaglic acid than other compounds especially high penetration depts. The photoelectric effect is in the neighborhood of proportional to $Z^{4-5}/E^{3.5}$. Compton scattering is dominant in the intermediate energy region and dependent on Z/E. All

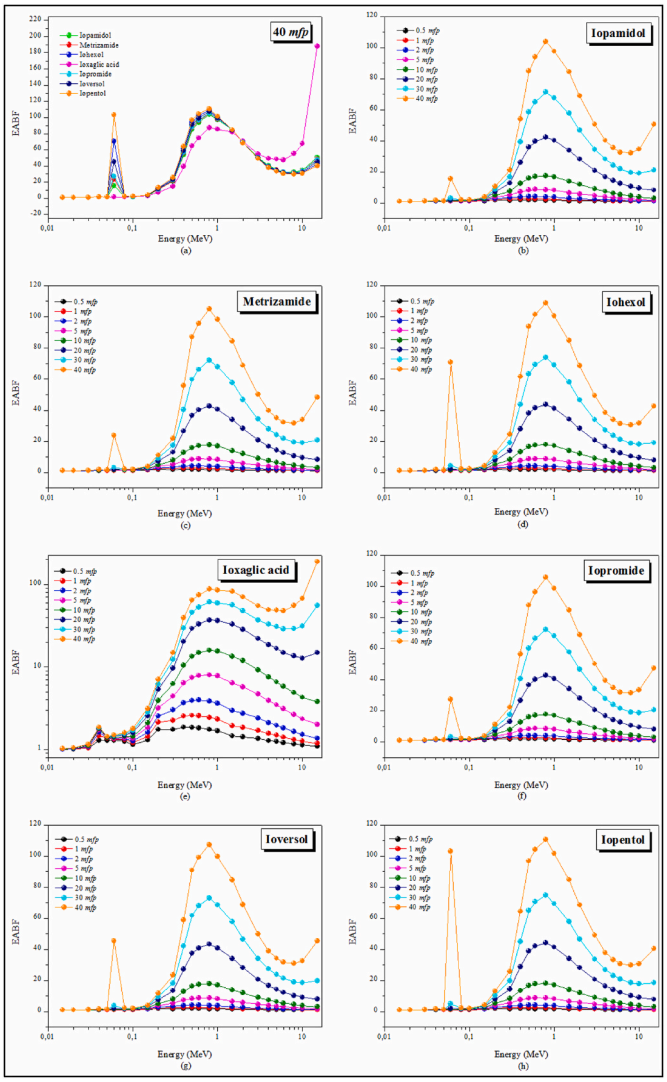

Fig. 6. *EABF* values of contrast agents in the energy region 0.015 MeV–15 MeV at 0.5, 1, 2, 5, 10, 20, 30 and 40 *mfp*.

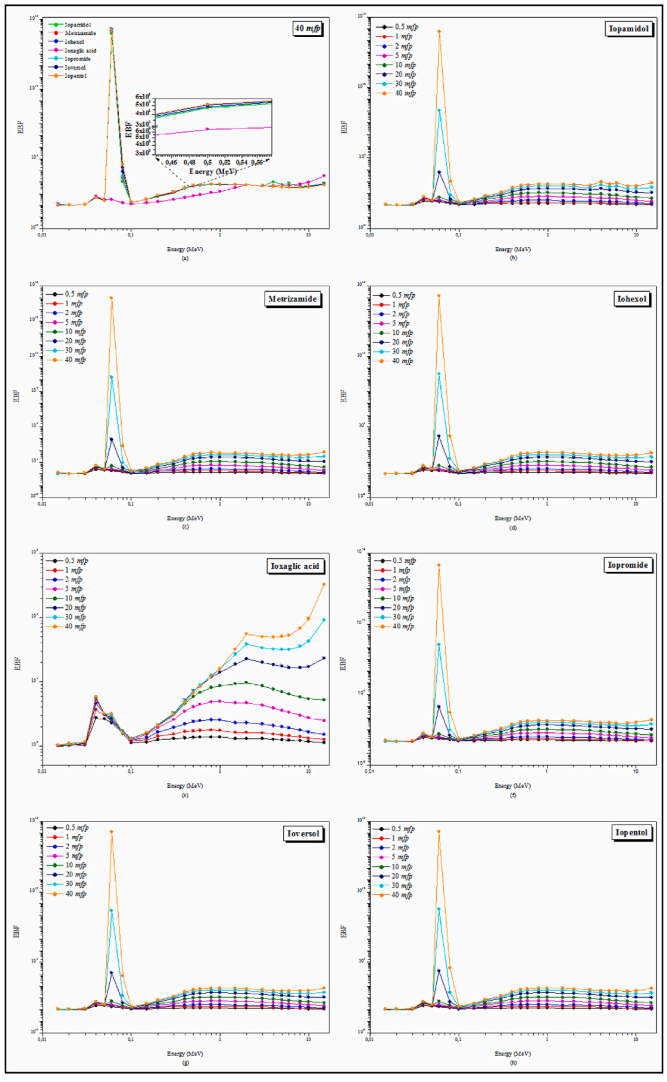

Fig. 7. *EBF* values of contrast agents in the energy region 0.015 MeV–15 MeV at 0.5, 1, 2, 5, 10, 20, 30 and 40 *mfp*.

contrast agents increased more slightly (except for Ioxaglic acid) with increasing photon energy in the high energy region. The highest *EABF* and *EBF* values at the high energy region among the contrast agents were belonged Ioxaglic acid. Compton scattering given place to pair production in high energy region and pair production is approximately dependent on Z^2. As seen from Table 7, Ioxaglic acid has the highest Z_{eqv} values especially high energy region. The reason for the highest energy absorption build-up factor values and exposure build-up factor values in the high energy region for Ioxaglic acid ($C_{24}H_{21}I_6N_5O_8$) is the highest Z_{eqv} values. *EABF* and *EBF* values for each contrast agent were increased with increasing mean free path values and taken the maximum values at 40 *mfp*. The values of *EABF* and *EBF* values showed similar behavior for many other materials such as glasses (Mahmoud et al., 2019; Kaur et al., 2019; Tekin et al., 2019), alloys (Manjunatha et al., 2019) and compounds (Yorgun and Kavaz, 2019; Oto et al., 2020).

EABF and *EBF* values of the Iopamidol, Metrizamide, Iohexol, Ioxaglic acid, Iopromide, Ioversol and Iopentol are plotted in Fig. 8(a–d) and 9 (a-d) against the penetration depth in the penetration depth region from 0.5 to 40 *mfp* at 0.015 MeV, 0.15 MeV, 1.5 MeV and 15 MeV photon energy. *EABF* and *EBF* values for each contrast agent were increased with increasing penetration depth. Ioxaglic acid took lowest *EABF* and *EBF* values at 0.015, 0.15 and 1.5 MeV photon energy among the contrast agents. In the high energy region, the *EABF* and *EBF* values showed an inverted trend and Ioxaglic acid took the highest *EABF* and *EBF* values at especially penetration depth 15 *mfp* $\leq$ PD $\leq$ 40 *mfp*. This situation can be explain that pair production is more dominant in the high energy region and as mentioned above pair production is approximately dependent on Z^2.

3.3. Results of kerma relative to air

Kerma relative to air values of a contrast agent were calculated from eq. (16) using the mass energy absorption coefficients taken from Hubbell and Seltzer (1995). Kerma relative to air values of the

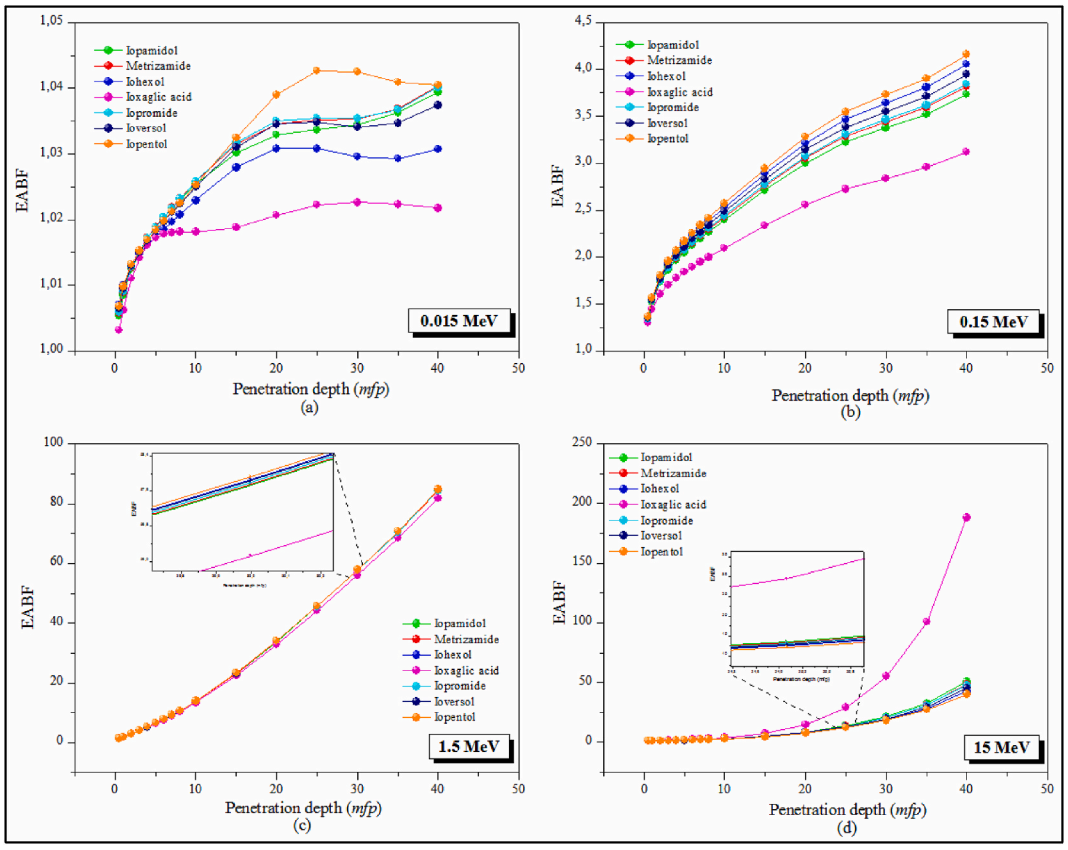

Fig. 8. *EABF* values of contrast agents up to 40 *mfp* at 0.015 MeV, 0.15 MeV, 1.5 MeV, 15 MeV.

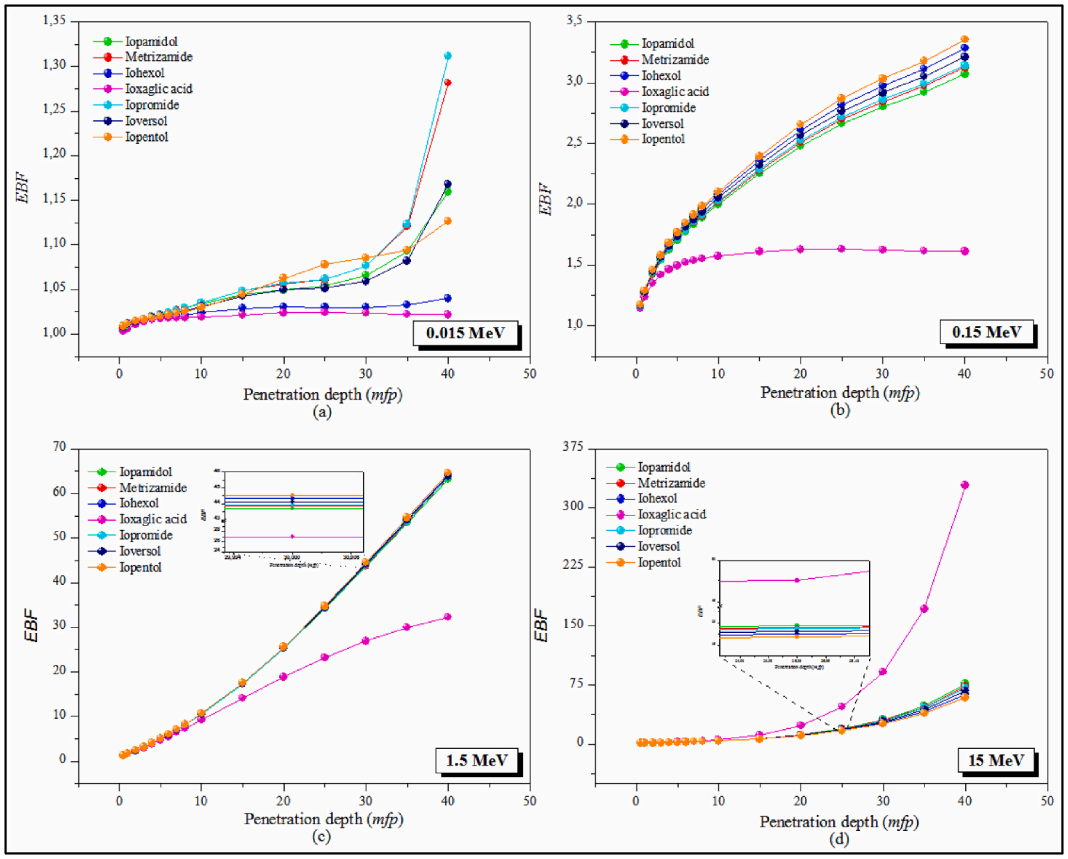

Fig. 9. *EBF* values of contrast agents up to 40 *mfp* at 0.015 MeV, 0.15 MeV, 1.5 MeV, 15 MeV.

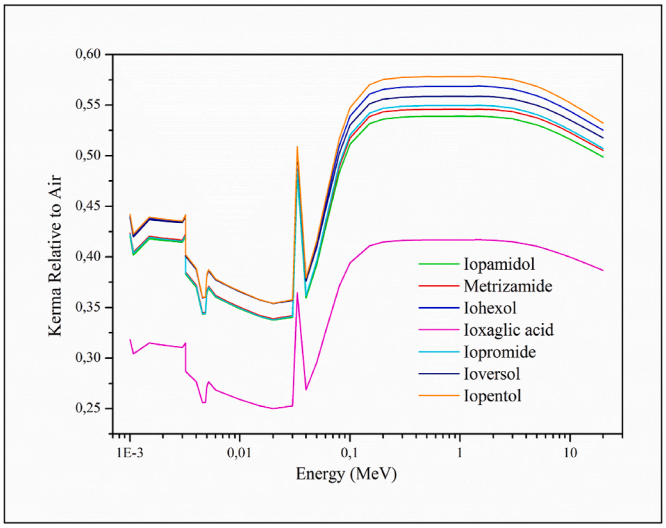

Fig. 10. Kerma relative to air values of contrast agents in the energy region 0.001 MeV–20 MeV.

Iopamidol, Metrizamide, Iohexol, Ioxaglic acid, Iopromide, Ioversol and Iopentol are plotted as a function of energy in the energy region 0.001 MeV $\leq$ E $\leq$ 20 MeV in Fig. 10. As seen from Fig. 10, Ioxaglic acid received the lowest kerma relative to air among the contrast agents. The contribution of the elements in the contrast agents is clearly seen from Fig. 10. For example, contribution of the Iodine in the contrast agents is clearly seen at the K shell edge energy of I (~0,033 MeV). As a result, it can be said that kerma relative to air values of the Iopamidol, Metrizamide, Iohexol, Ioxaglic acid, Iopromide, Ioversol and Iopentol are depent on the chemical composition of the contrast agents and photon energy just like other radiation attenuation parameters.

4. Conclusion

In this study, μ/ρ, μ, *HVL*, *TVL*, *mfp*, Z_{Eff} and N_{Eff} values were determined in the energy range from 60 keV to 15 MeV for Iopamidol, Metrizamide, Iohexol, Ioxaglic acid, Iopromide, Ioversol and Iopentol. *EABF* and *EBF* values were calculated in the energy region 0.015 MeV $\leq$ E $\leq$ 15 MeV for penetration depths up to 40 *mfp* for contrast agents. Important variations were observed on attenuation parameters. Also, kerma relative to air values for the contrast agents were investigated in the energy region 0.001 MeV $\leq$ E $\leq$ 20 MeV. All parameters appeared to support each other. As shown in tables and figures, Ioxicid acid is a good radiation absorber according to the other studied contrast agents. The number of studies is very limited in the literature for the attenuation parameters on contrast agents. The present results may contribute to various application areas of radiation research especially medicine and pharmacy.

Declaration of competing interest

No potential conflict of interest was reported by the author.

References

Agostinelli, S., Allison, J., Amako, K.A., Apostolakis, J., Araujo, H., Arce, P., Asai, M., Axen, D., Banerjee, S., Barrand, G.2., Behner, F., 2003. Geant4 Collaboration. GEANT4—a simulation toolkit. Nucl. Instrum. Methods Phys. Res., Sect. A 506 (3), 250–303.

Akman, F., Kaçal, M.R., Sayyed, M.I., Karataş, H.A., 2019a. Study of gamma radiation attenuation properties of some selected ternary alloys. J. Alloys Compd. 782, 315–322.

Akman, F., Khattari, Z.Y., Kaçal, M.R., Sayyed, M.I., Afaneh, F., 2019b. The radiation shielding features for some silicide, boride and oxide types ceramics. Radiat. Phys. Chem. 160, 9–14.

Al-Buriahi, M.S., Tonguc, B.T., 2020. Mass attenuation coefficients, effective atomic numbers and electron densities of some contrast agents for computed tomography. Radiat. Phys. Chem. 166, 108507.

ANSI/ANS-6.4.3, 1991. Gamma Ray Attenuation Coefficient and Buildup Factors for Engineering Materials. American Nuclear Society, La Grange Park, IL, USA.

Attix, F.H., 1986. Introduction to Radiological Physics and Radiation Dosimetry (Chapter 2), Page 22. WILEY-VCH Verlag GmbH & Co. KGaA.

Aygün, B., Şakar, E., Cinan, E., Yorgun, N.Y., Sayyed, M.I., Agar, O., Karabulut, A., 2020. Development and production of metal oxide doped glasses for gamma ray and fast neutron shielding. Radiat. Phys. Chem. 174, 108897.

Chen, S., Chai, Z., Xue, D., Jiang, X., Yang, Y., 2018. Variation of gamma radiation shielding properties with incident photon energy and penetration depth for WC/Al composites. Radiat. Eff. Defect Solid 173, 399–413.

Çakır, T., 2020. Determining the photon interaction parameters of iodine compounds as contrast agents for use in radiology. J. Radiat. Res. Appl. Sci. 13 (1), 252–259.

Ekinci, N., Kavaz, E., Özdemir, Y., 2014. A study of the energy absorption and exposure buildup factors of some anti-inflammatory drugs. Appl. Radiat. Isot. 90, 265–273.

Eng, J., Subramaniam, R.M., Wilson, R.F., Turban, S., Choi, M.J., Zhang, A., Suarez-Cuervo, C., Sherrod, C., Hutfless, S., Iyola, E.E., Bass, E.B., 2015. Contrast-Induced Nephropathy: Comparative Effects of Different Contrast Media, vol. 15. AHRQ Publication No. (16), EHC022-EF.

Gerward, L., Guilbert, N., Jensen, K.B., Levring, H., 2004. WinXCom –a program for calculating X-ray attenuation coefficients. Radiat. Phys. Chem. 71, 653–654.

Hubbell, J.H., Seltzer, S.M., 1995. Tables of X-Ray Mass Attenuation Coefficients and Mass Energy-Absorption Coefficients 1 keV to 20 MeV for Elements Z= 1 to 92 and 48 Additional Substances of Dosimetric Interest. National Institute of Standards and Physics Laboratory, NISTIR, p. 5632.

Issa, S.A.M., Sayyed, M.I., Zaid, M.H.M., Matori, K.A., 2018. Photon parameters for gamma-rays sensing properties of some oxide of lanthanides. Results Phys 9, 206–210.

Kaçal, M.R., Akman, F., Sayyed, M.I., Akman, F., 2019. Evaluation of gamma-ray and neutron attenuation properties of some polymers. Nucl. Eng. Technol. 51, 818–824.

Kaur, P., Singh, K.J., Kurudirek, M., Thakur, S., 2019. Study of environment friendly bismuth incorporated lithium borate glass system for structural, gamma-ray and fast neutron shielding properties. Spectrochim. Acta, Part A 223, 117309.

Kavaz, E., Perişanoğlu, U., Ekinci, N., Özdemir, Y., 2016. Determination of energy absorption and exposure buildup factors by using G-P fitting approximation for radioprotective agents. Int. J. Radiat. Biol. 92 (7), 380–387.

Kökpınar, B., Öztürk, B.C., Çam, N.F., Akat, H., 2020. Radiation shielding properties of Poly(hydroxylethyl methacrylate)/Tungsten(VI) oxide composites. Mater. Chem. Phys. 239, 121986.

Kurudirek, M., Doğan, M., İngeç, M., Ekinci, N., Özdemir, Y., 2011. Gamma-ray energy absorption and exposure buildup factor studies in some human tissues with endometriosis. Appl. Radiat. Isot. 69, 381–388.

Kurudirek, M., 2014. Photon buildup factors in some dosimetric materials for heterogeneous radiation sources. Radiat. Environ. Biophys. 53, 175–185.

Mahmoud, S.I., Issa, S.A.M., Saddeek, Y.B., Tekin, H.O., Kilicoglu, O., Alharbi, T., Sayyed, M.I., Erguzel, T.T., Elsaman, R., 2019. Gamma, neutron shielding and mechanical parameters for lead vanadate glasses. Ceram. Int. 45, 14058–14072.

Manjunatha, H.C., Rudraswamy, B., 2012. Energy absorption and exposure build-up factors in hydroxyapatite. Radiat. Meas. 47, 364–370.

Manjunatha, H.C., Sathish, K.V., Seenappa, L., Gupta, D., Raj, A.C., 2019. A study of X-ray, gamma and neutron shielding parameters in Si- alloys. Radiat. Phys. Chem. 165, 108414.

Oto, B., Kavaz, E., Durak, H., Aras, A., Madak, Z., 2019. Effect of addition of molybdenum on photon and fast neutron radiation shielding properties in ceramics. Ceram. Int. 45, 23681–23689.
Oto, B., Oto, G., Madak, Z., Kavaz, E., 2020. The interaction of gamma radiation with drugs used in cholinergic medications. Int. J. Radiat. Biol. 96 (2), 236–244.
Saleh, H.H., Sharaf, J.M., Alkhateeb, S.B., Hamideen, M.S., 2019. Studies on equivalent atomic number and photon buildup factors for some tissues and phantom materials. Int. J. Radiat. Phys. Chem. 165, 108388.
Sayyed, M.I., 2016. Investigation of shielding parameters for smart polymers. Chin. J. Phys. 54, 408–415.
Sayyed, M.I., Akman, F., Kaçal, M.R., 2019. Experimental investigation of photon attenuation parameters for different binary alloys. Radiochim. Acta 107 (4), 339–348.
Singh, V.P., Badiger, N.M., 2016. Studies on photon buildup for some thermoluminescent dosimetric compounds. Indian J. Phys. 90 (3), 259–269.
Singh, R., Singh, D., Singh, A., Dhaliwal, A.S., 2019. Photon interaction parameters investigations for some $ZnO–Al_2O_3–Fe_2O_3–P_2O_5$ glasses at 59.4 keV incident photon energy. Glass Phys. Chem. 45 (3), 202–207.
Tekin, H.O., Kassab, L.R.P., Issa, S.A.M., Bordon, C.D.S., Altunsoy Guclu, E.E., da Silva Mattos, G.R., Kilicoglu, O., 2019. Synthesis and nuclear radiation shielding characterization of newly developed germanium oxide and bismuth oxide glasses. Ceram. Int. 45, 24664–24674.
Yorgun, N.Y., Kavaz, E., 2019. Gamma photon protection properties of some cancer drugs for medical applications. Results Phys 13, 102150.